ADVANCED ELECTRONIC MATERIALS

Supporting Information

for *Adv. Electron. Mater.,* DOI: 10.1002/aelm.202100802

Beneficial Effect of Na_2CO_3 Additions on the Thermoelectric Performance of Melt-Route Cu_2Se

Sheik Md Kazi Nazrul-Islam, Md Rezoanur Rahman, Al Jumlat Ahmed, Frank Fei Yun, David L. Cortie, Xiaolin Wang,* and Michael B. Cortie**

Supporting Information

Beneficial effect of Na_2CO_3 additions on the thermoelectric performance of melt-route Cu_2Se

Sheik Md Kazi Nazrul Islam[*], *Md Rezoanur Rahman, Al Jumlat Ahmed, Frank Fei Yun, David L. Cortie, Xiaolin Wang*[*], *Michael B. Cortie*[*]

Table S1. Parameters for the refinement of pure Cu_2Se and Na_2CO_3 incorporated Cu_2Se samples at room temperature. R_p and R_{wp} are the profile and weighted profile R-factors, respectively, χ^2 is the goodness-of-fit, and Derived Bragg R-Factor.

	a (Å)	b (Å)	c (Å)	β (°)	V (Å^3)	R_p	R_{wp}	χ^2	DERIVED BRAGG R-FACTOR
Cu_2Se	7.13304 ± 0.0009	12.36786 ± 0.0014	27.34226 ± 0.0031	94.34507 ± 0.0099	2405.211 ± 0.5035	4.95	6.46	0.06	2.36
0.09 wt.% Na_2CO_3	7.13457 ± 0.0013	12.36909 ± 0.0025	27.34171 ± 0.0055	94.33521 ± 0.0087	2405.952 ± 0.8150	4.63	6.07	0.05	2.00
0.18 wt.% Na_2CO_3	7.13374 ± 0.0010	12.37004 ± 0.0018	27.34909 ± 0.0040	94.34977 ± 0.0084	2406.46 ± 0.6068	4.46	5.82	0.05	2.06
0.35 wt.% Na_2CO_3	7.13345 ± 0.0015	12.37146 ± 0.0028	27.35002 ± 0.0062	94.35077 ± 0.0087	2406.717 ± 0.9100	4.71	6.12	0.05	2.30
0.70 wt.% Na_2CO_3	7.13683 ± 0.0009	12.37408 ± 0.0014	27.37454 ± 0.0031	94.3719 ± 0.0096	2410.457 ± 0.4916	4.76	6.23	0.06	2.51
1.40 wt.% Na_2CO_3	7.13944 ± 0.0010	12.37765 ± 0.0014	27.38372 ± 0.0034	94.37183 ± 0.0101	2412.842 ± 0.5282	4.9	6.37	0.06	2.93

Table S2. Parameters for the refinement of pure Cu_2Se and Na_2CO_3 incorporated Cu_2Se samples at 398 K, 448 K, 498 K, 548 K, 648 K, and 747 K. R_p and R_{wp} are the profile and weighted profile R-factors, respectively, χ^2 is the goodness-of-fit, and Derived Bragg R-Factor.

Temp (K)	Lattice parameter / Sample	a (Å)	R_p	R_{wp}	χ^2	DERIVED BRAGG R-FACTOR
398	1.40 wt% Na_2CO_3	5.8126 ±0.0004	8.58	11.2	1.20	0.96
448		5.8202 ±0.0003	8.68	11.24	1.21	0.75
498		5.8282 ±0.0002	8.95	11.69	1.31	0.54
548		5.8354 ±0.0002	8.52	11.75	1.95	3.44
648		5.8515 ±0.0001	9.9	12.9	1.56	5.34
747		5.8669 ±0.0001	8.88	12	1.98	7.07
397	Cu_2Se	5.8026 ±0.0003	7.58	10.46	1.69	0.71
447		5.8099 ±0.0003	7.78	10.49	1.663	0.83
497		5.8170 ±0.0002	7.91	10.76	1.713	0.89
548		5.8258 ±0.0001	7.51	10.34	2.05	2.61
646		5.8408 ±0.0001	9.42	12.61	2.32	2.63
747		5.8594 ±0.0001	9.76	13.34	2.538	3.35

Table S3. Effect0 of heat treatment on the room temperature lattice parameters of the sample aliquots run through the DSC (not physically the same samples as in Table S1). Whereas there is no statistically significant difference in *a*, *b* or *c* before and after the heat treatment, there is a consistent small decrease in γ.

% Na_2CO_3	before heat-treatment				after thermal cycle			
	a	b	c	γ	a	b	c	γ
0.00	7.133 ± 0.004	12.365 ± 0.005	27.336 ± 0.006	94.33 ± 0.04	7.134 ± 0.001	12.368 ± 0.001	27.338 ± 0.001	94.28 ± 0.01
0.09	7.132 ± 0.004	12.365 ± 0.006	27.336 ± 0.014	94.33 ± 0.04	7.130 ± 0.001	12.361 ± 0.001	27.332 ± 0.001	94.30 ± 0.01
0.18	7.129 ± 0.004	12.365 ± 0.006	27.329 ± 0.012	94.32 ± 0.04	7.128 ± 0.001	12.358 ± 0.001	27.309 ± 0.001	94.27 ± 0.01
0.35	7.128 ± 0.004	12.360 ± 0.006	27.317 ± 0.006	94.32 ± 0.04	7.127 ± 0.001	12.356 ± 0.001	27.304 ± 0.002	94.28 ± 0.01
0.70	7.134 ± 0.004	12.371 ± 0.006	27.361 ± 0.006	94.35 ± 0.04	7.128 ± 0.001	12.360 ± 0.001	27.316 ± 0.001	94.28 ± 0.01
1.40	7.132 ± 0.004	12.366 ± 0.006	27.349 ± 0.005	94.35 ± 0.04	7.135 ± 0.001	12.369 ± 0.001	27.366 ± 0.001	94.31 ± 0.01

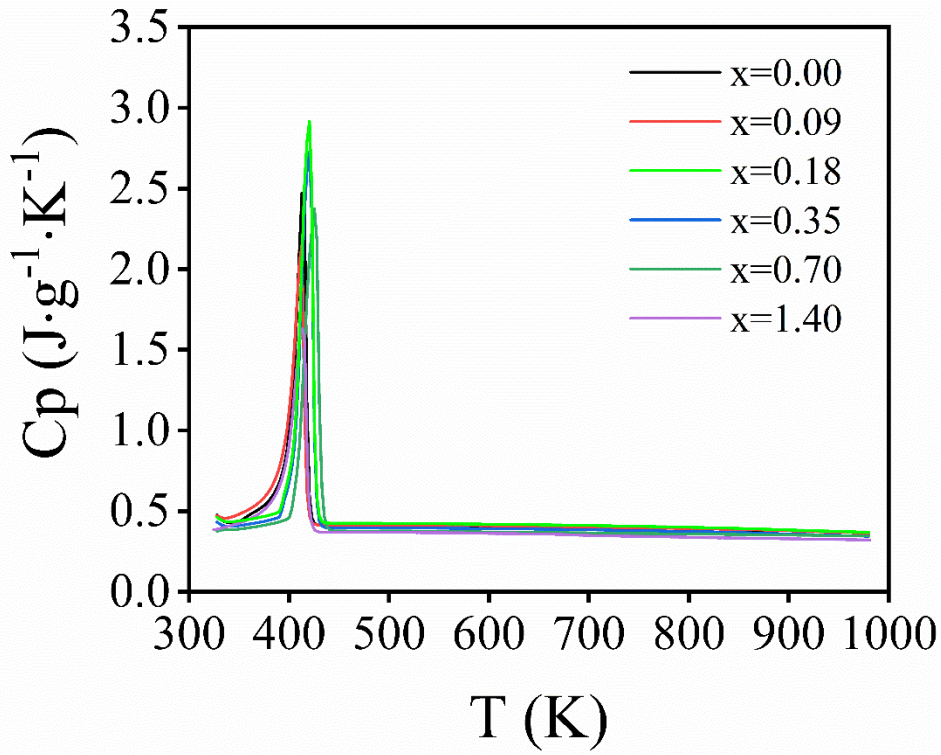

Figure S1. Temperature dependence of heat capacity (C_p) for different additions of Na_2CO_3 to Cu_2Se.

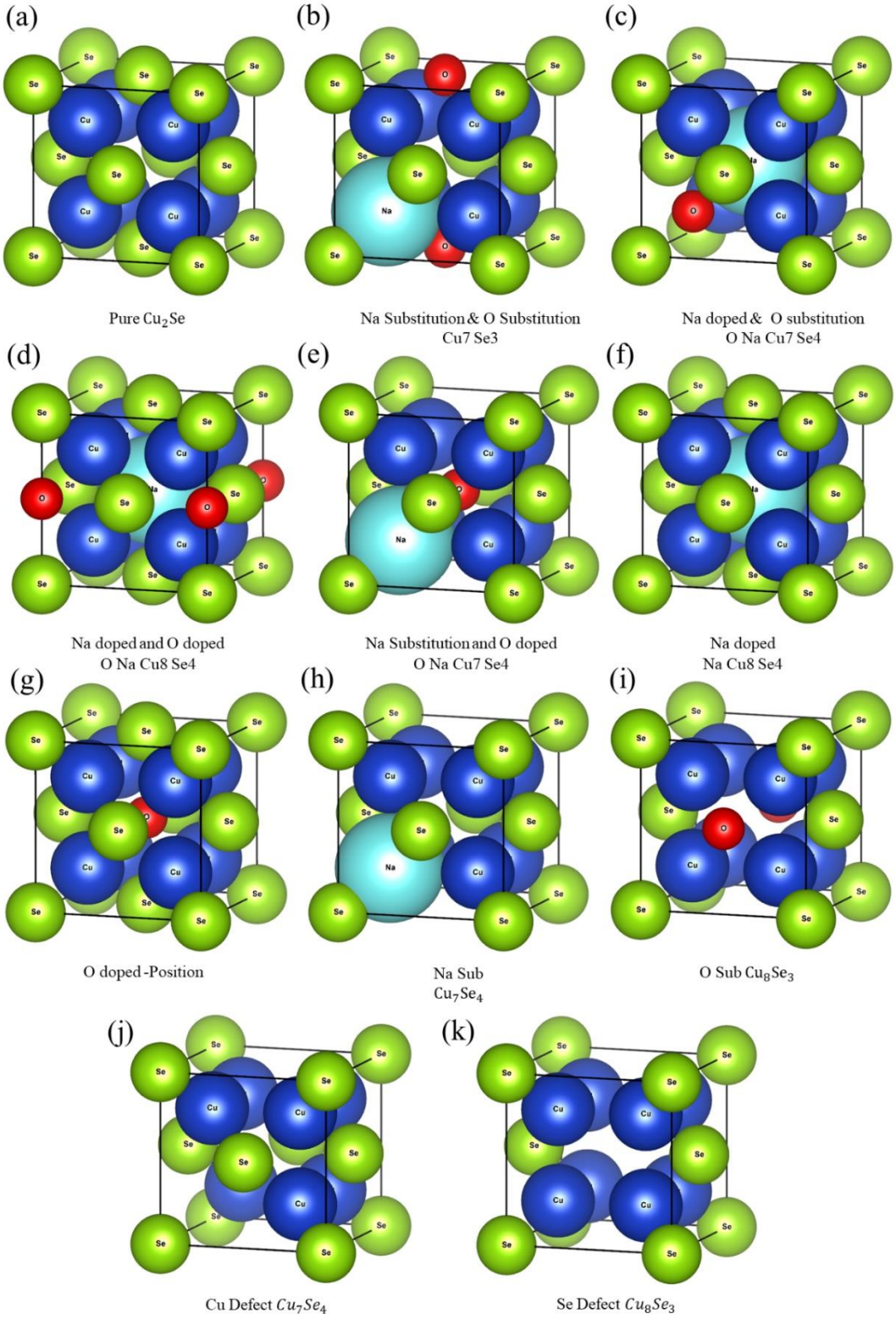

Figure S2. Unit cell of (a) stoichiometric Cu_2Se; (b) Na O Cu_7 Se_3 (Na Substitution and O Substitution); (c) O Na Cu_7 Se_4 (Na doped and O substitution); (d) O Na Cu_8 Se_4 (Na doped and O doped); (e) O Na Cu_7 Se_4 (Na Substitution and O doped); (f) Na Cu_8 Se_4 (Na doped); (g) O Cu_8 Se_4 (O doped); (h) Na Cu_7 Se_4 (Na substitute); (i) O Cu_8 Se_3 (O substitute); (j) Cu_7 Se_4 (Cu defect); (k) Cu_8 Se_3 (Se defect); (l) Cu_8 Se_4 (Na_2O defect).

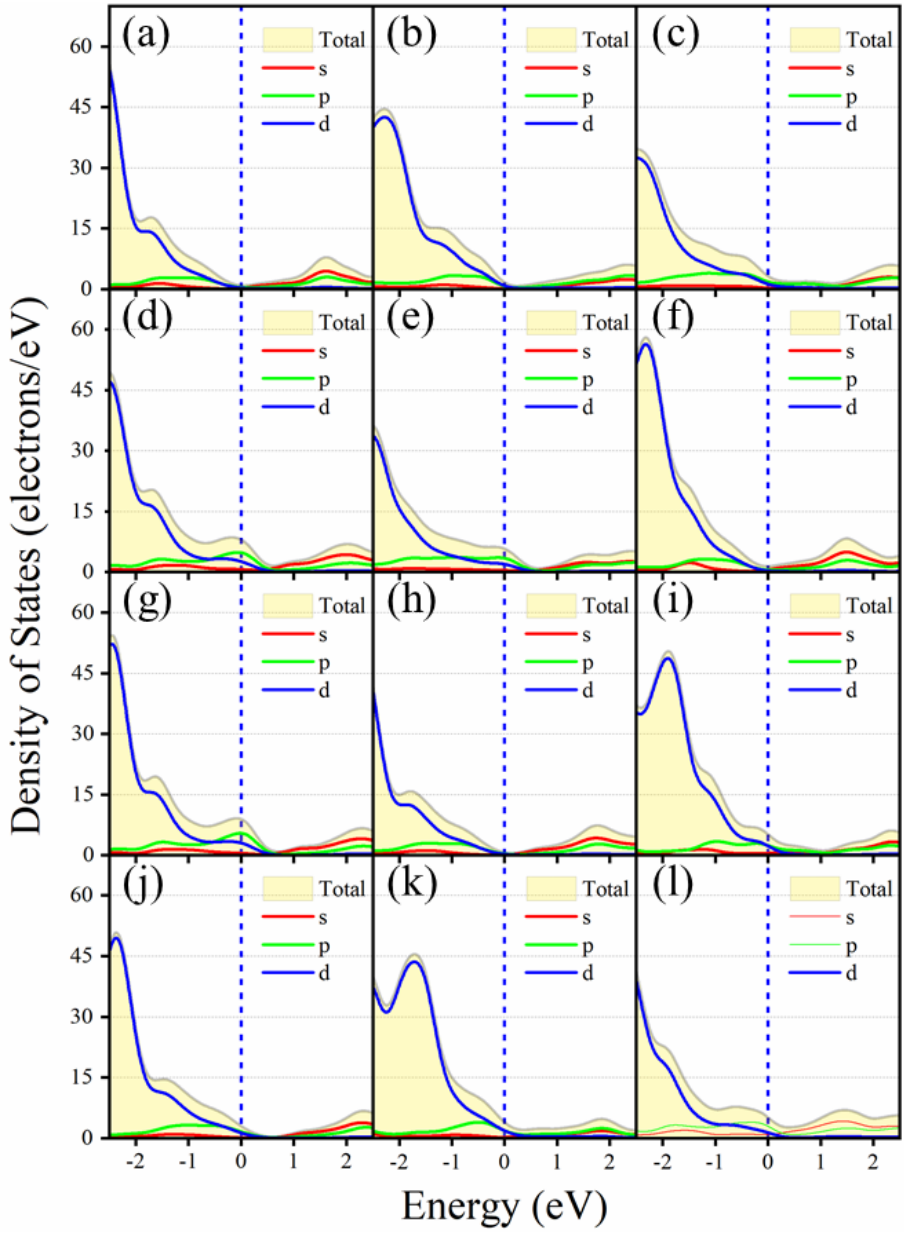

Figure S3. Calculated total and partial electronic density of states (DOS) for the stoichiometric Cu_2Se and Cu_2Se with Na and/or O compounds obtained from the Density Functional Theory calculations. (a) total and partial DOS for the Cu_2Se; (b) total and partial DOS for the Na O Cu_7 Se_3 (Na Substitution and O Substitution); (c) total and partial DOS for the O Na Cu_7 Se_4 (Na doped and O substitution); (d) total and partial DOS for the O Na Cu_8 Se_4 (Na doped and O doped); (e) total and partial DOS for the O Na Cu_7 Se_4 (Na Substitution and O doped); (f) total and partial DOS for the Na Cu_8 Se_4 (Na doped); (g) total and partial DOS for the O Cu_8 Se_4 (O doped); (h) total and partial DOS for the Na Cu_7 Se_4 (Na substitute); (i) total and partial DOS for the O Cu_8 Se_3 (O substitute); (j) total and partial DOS for the Cu_7 Se_4 (Cu defect); (k) total and partial DOS for the Cu_8 Se_3 (Se defect); (l) total and

partial DOS for the Cu_8 Se_4 (Na_2O defect). The vertical lines mark the position of the Fermi level (E_F).

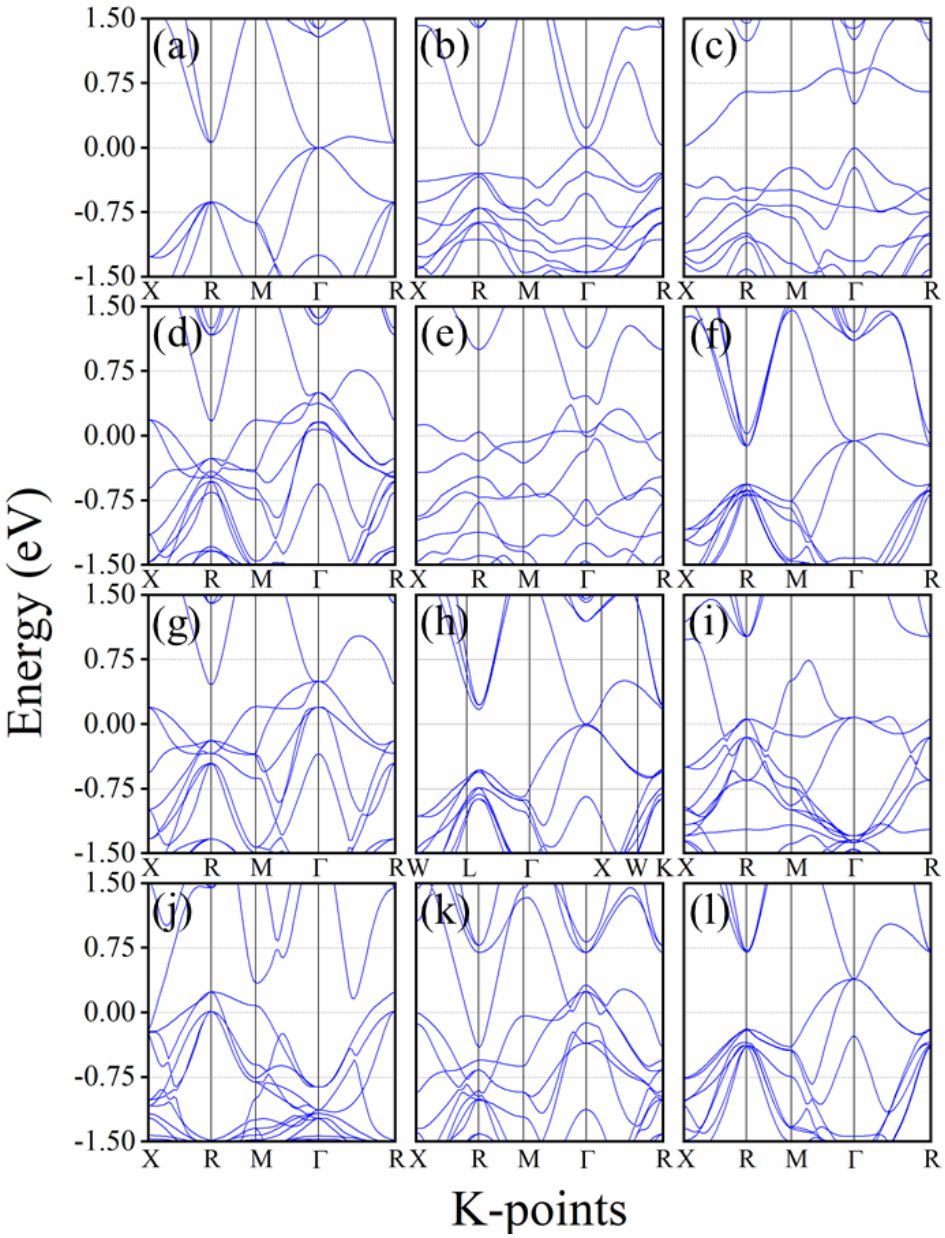

Figure S4. Calculated band structure for the stoichiometric Cu_2Se and Cu_2Se with Na and/or O compounds obtained from the Density Functional Theory calculations. (a) Calculated band structure for the Cu_2Se; (b) Calculated band structure for the Na O Cu_7 Se_3 (Na Substitution and O Substitution); (c) Calculated band structure for the O Na Cu_7 Se_4 (Na doped and O substitution); (d) Calculated band structure for the O Na Cu_8 Se_4 (Na doped and O doped); (e) Calculated band structure for the O Na Cu_7 Se_4 (Na Substitution and O doped); (f) Calculated band structure for the Na Cu_8 Se_4 (Na doped); (g) Calculated band structure for the O Cu_8 Se_4 (O doped); (h) Calculated band structure for the Na Cu_7 Se_4 (Na substitute); (i) Calculated band structure for the O Cu_8 Se_3 (O substitute); (j) Calculated band structure for the Cu_7 Se_4 (Cu defect); (k) Calculated band structure for the Cu_8 Se_3 (Se defect); (l) Calculated band structure for the Cu_8 Se_4 (Na_2O defect).

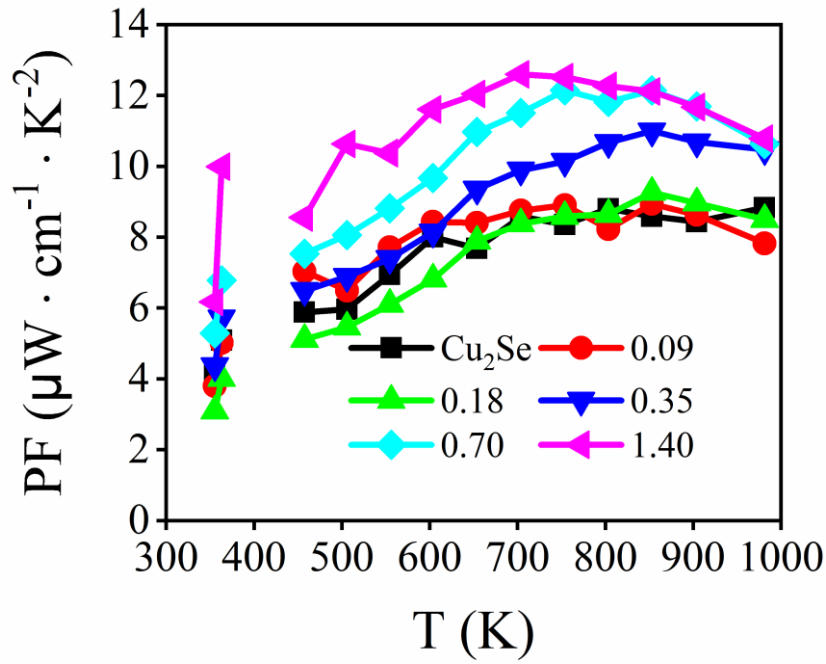

Figure S5. Temperature dependent power factor of the Cu_2Se-xwt. % Na_2CO_3 samples (x = 0, 0.09, 0.18, 0.35, 0.70, and 1.40.

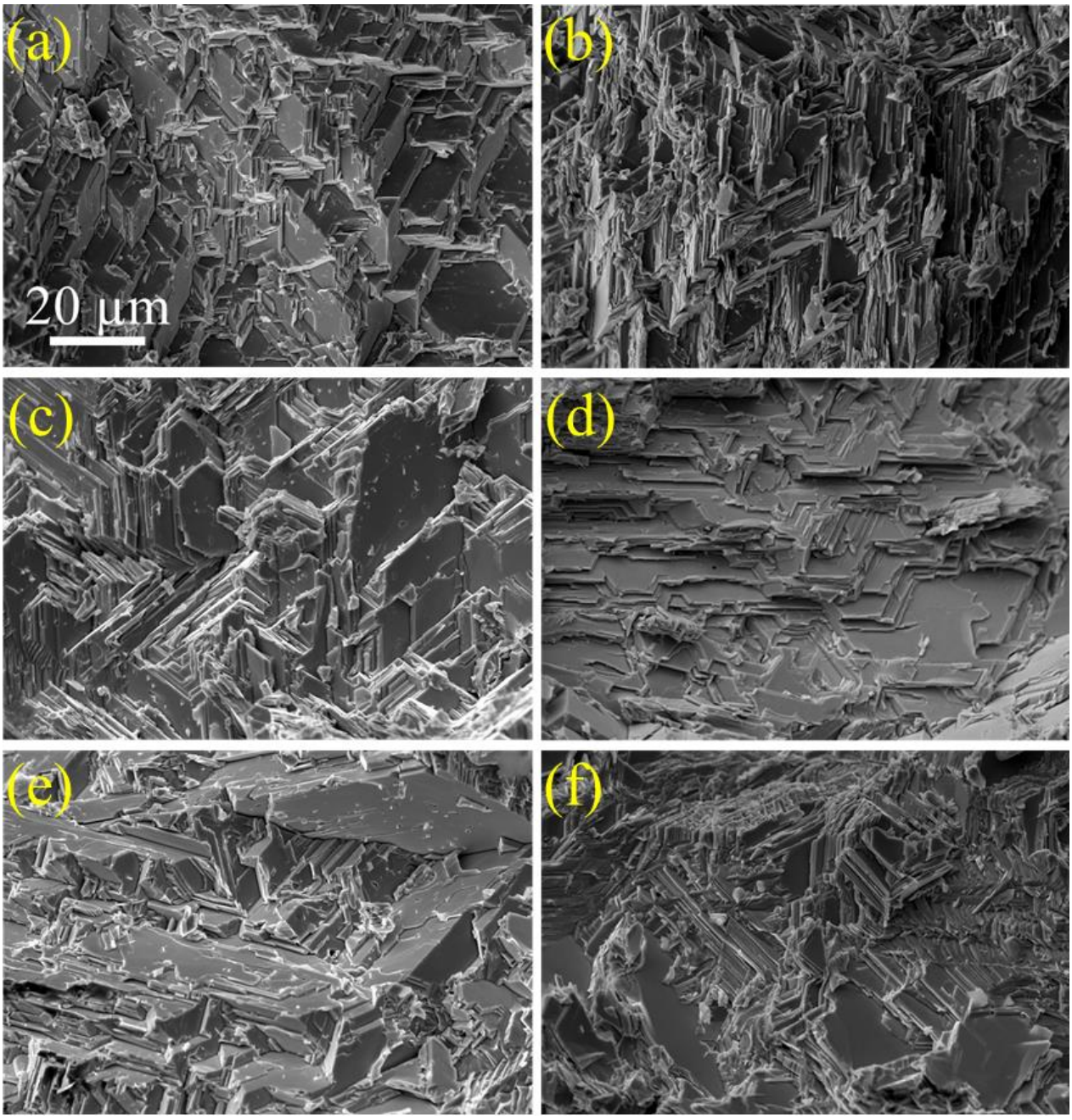
(a)
20 µm
(b)
(c)
(d)
(e)
(f)

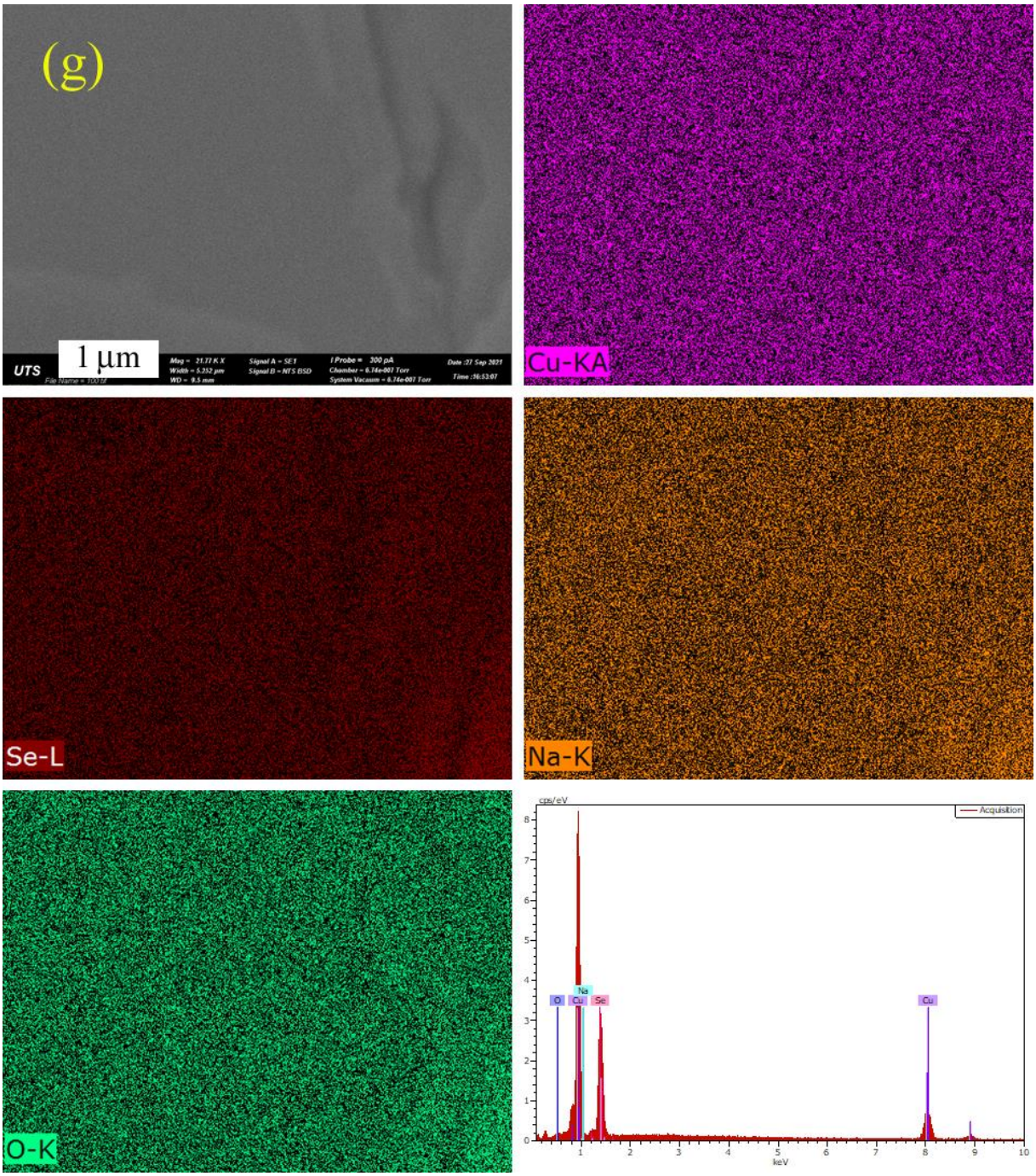

Figure S6. Freshly fractured cross sectioned image of (a) pure Cu_2Se; (b) 0.09 wt.% Na_2CO_3; (c) 0.18 wt.% Na_2CO_3; (d) 0.35 wt.% Na_2CO_3; (e) 0.70 wt.% Na_2CO_3 and (f) 1.40 wt.% Na_2CO_3 samples (g) EDS mapping showing homogenous composition at magnification used here (about 10,000 × on page).

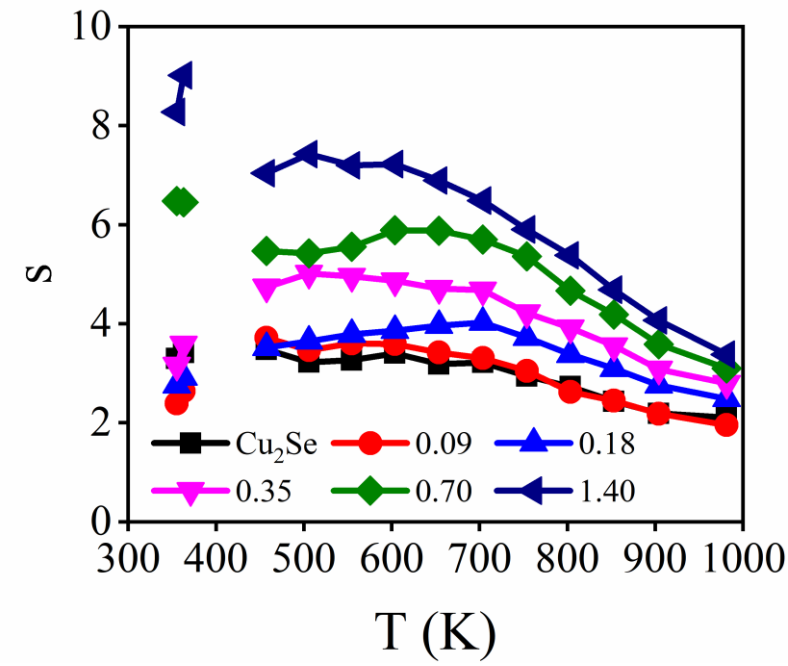

Figure S7. Temperature dependent compatibility factors of the Cu_2Se-*x* wt.% Na_2CO_3 samples (*x* = 0, 0.09, 0.18, 0.35, 0.70, and 1.40).

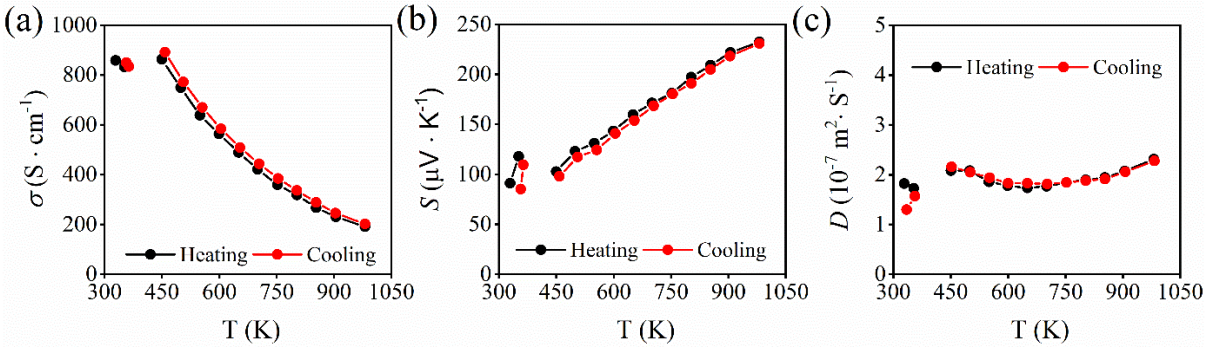

Figure S8. The electrical and thermal transport properties with respect to temperature during heating up and cooling down for a 1.40 wt.% Na_2CO_3 incorporated Cu_2Se sample: (a) electrical conductivity (σ); (b) Seebeck coefficient (*S*); (c) thermal diffusivity (*D*).

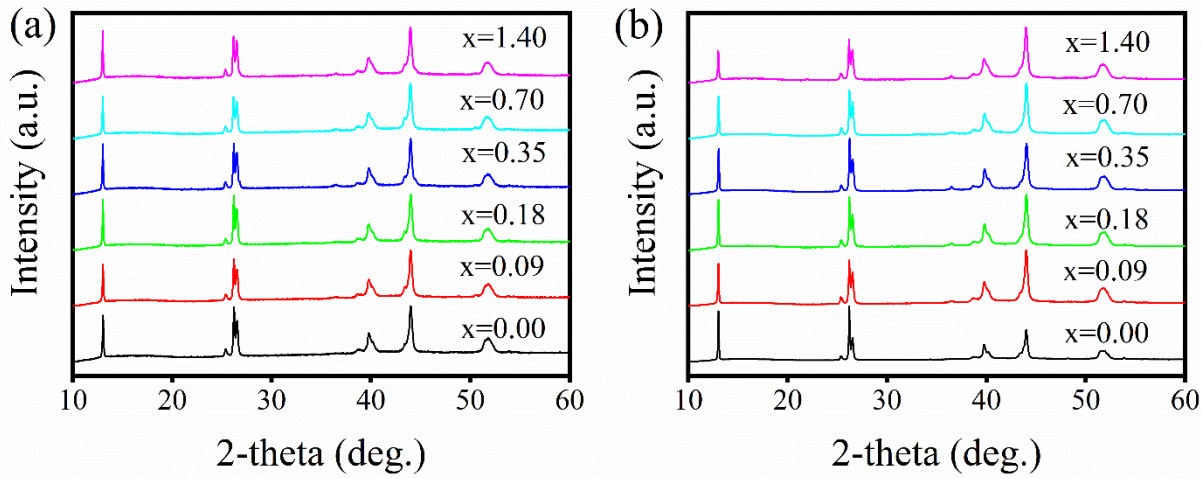

Figure S9. Room temperature powder x-ray diffraction pattern (a) before thermal cycle (b) after thermal cycle of samples (x = 0, 0.09, 0.18, 0.35, 0.70, and 1.40). See Table S3 for further analysis.

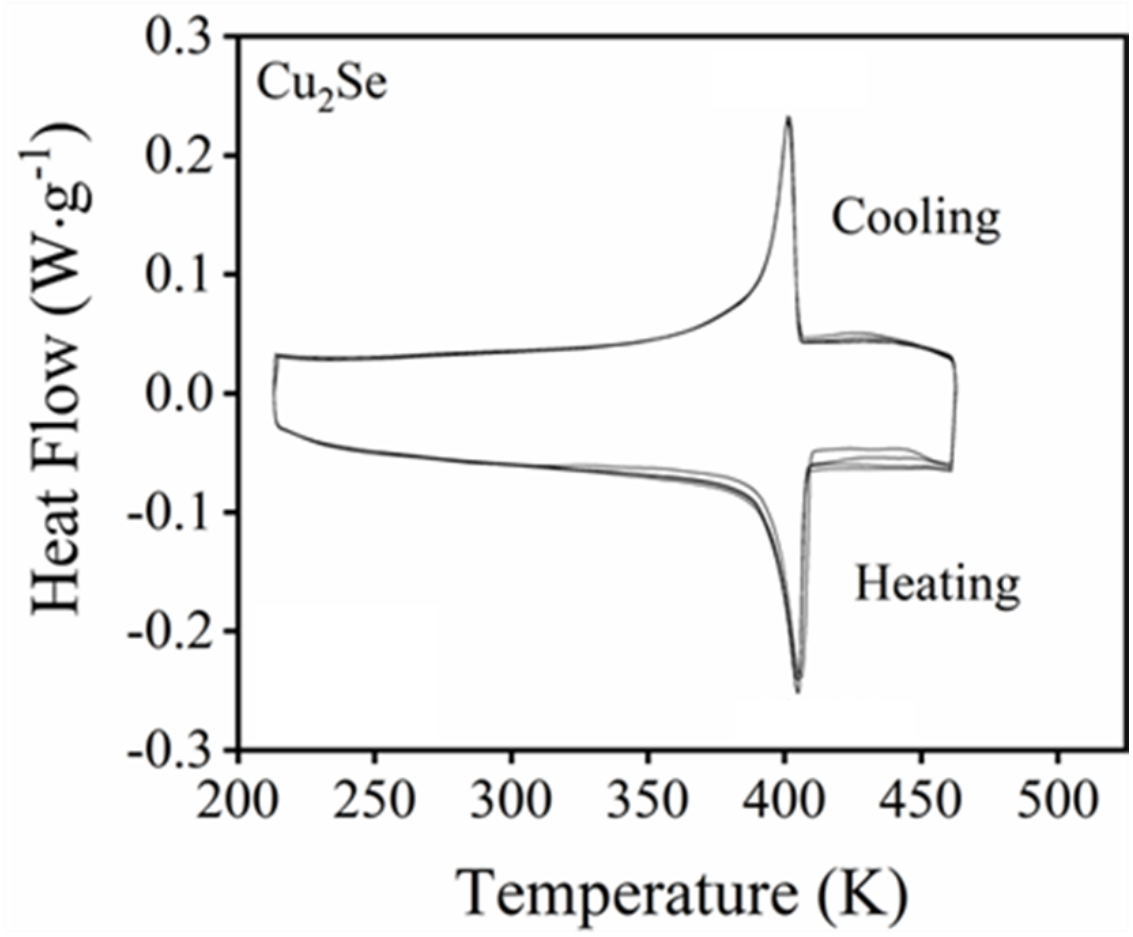

Figure S10. DSC thermogram of Cu_2Se powder with 4 heating–cooling cycles (5 °C/min).

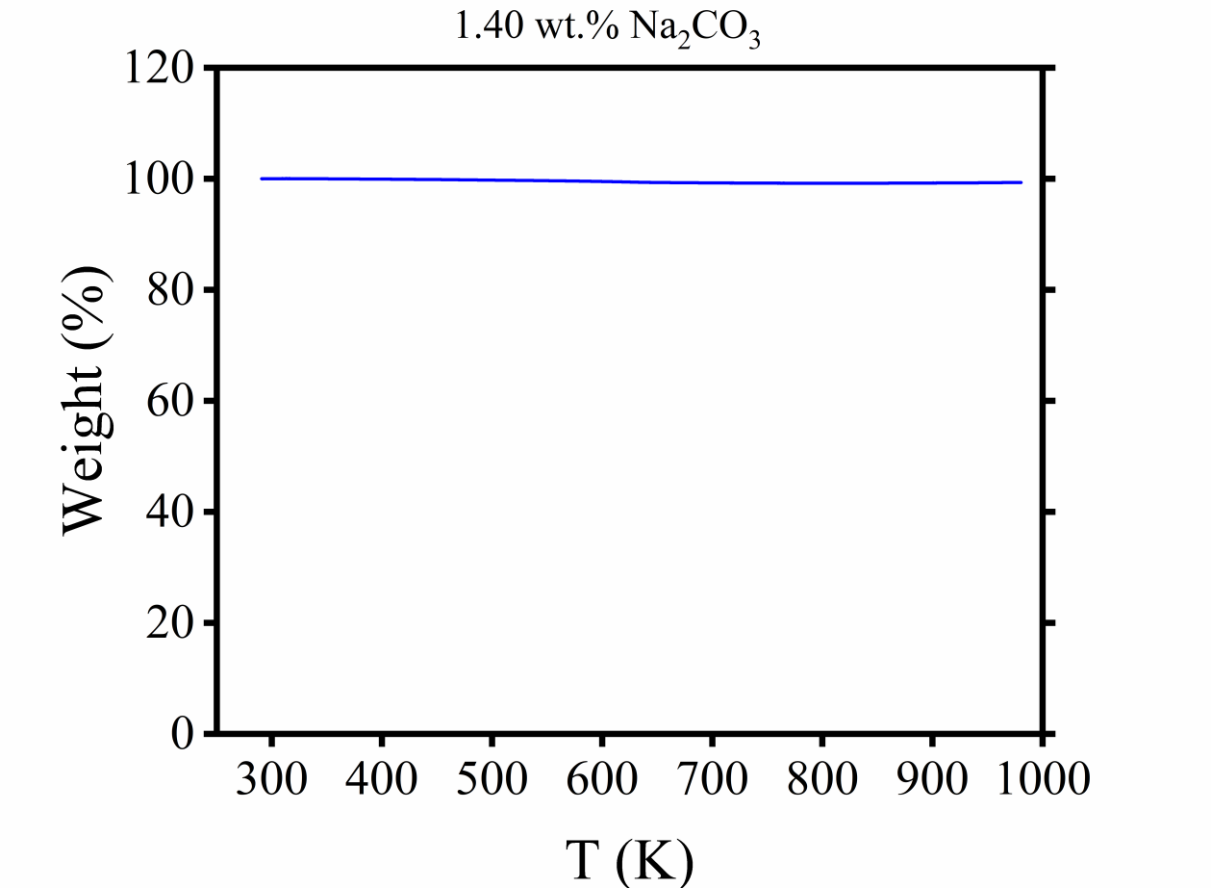

Figure S11. Thermogravimetric scan of a sample of Na-doped Cu_2Se run in an atmosphere of nitrogen. There is a mass loss of ~0.6 %. This indicates that the surface of a Cu_2Se device needs to be protected from evaporation of Se and/or oxidation.